AD-A085 975 BAYLOR COLL OF MEDICINE HOUSTON TX F/G 6/3
BIOPHYSICAL STUDY OF NERVE AXON.(U)
FEB 80 D C CHANG N00014-77-C-0092
UNCLASSIFIED NL

END
DATE FILMED
8 80
DTIC

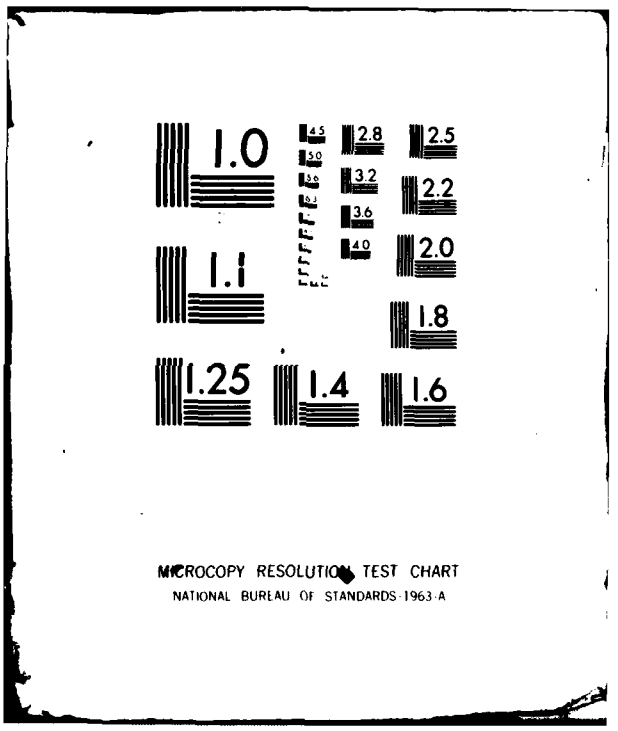
1.0
1.1
1.25
1.4
1.6
1.8
2.0
2.2
2.5
2.8
3.2
3.6
4.0
4.5
5.0
MICROCOPY RESOLUTION TEST CHART
NATIONAL BUREAU OF STANDARDS-1963-A

(12) SC

(9) FINAL REPORT 1 Jan 77 - 29 Feb 80

TITLE OF RESEARCH: BIOPHYSICAL STUDY OF NERVE AXON.

(15) ONR CONTRACT NO. N00014-77-C-0092

JANUARY 1, 1977 - FEBRUARY 29, 1980

(12) 13

By

(11) [illegible]

(10) DONALD C. CHANG, Ph.D.

Source : Baylor College of Medicine
Houston, Texas 77030

FINAL REPORT

This report summarizes research on the following topics:

1. **Study of Resting Potential in Squid Giant Axon-- Evidence Against the Diffusion Potential Hypothesis.**

Among the many theories proposed to explain the origin of the cellular potential, the hypothesis of diffusion potential is the most widely recognized one. This theory proposes that the cytoplasm is similar to that of a dilute electrolyte solution, and the resting potential is determined by the ionic permeabilities of the cell membrane which separates the intracellular and extracellular compartments. By using an assumption of constant field, the Goldman equation was derived to relate the resting potential with the ionic concentration gradients. We have conducted two experiments in squid giant axon to test the validity of this diffusion potential hypothesis. Firstly, we studied the resting potential as a function of internal potassium concentration. Secondly, we studied the effect of external sodium concentration on the resting potential. We found that: (1) contrary to the expectation of the diffusion potential hypothesis, the change of the internal potassium concentration has a much smaller effect on the resting potential than the change of the external potassium concentration. In fact, a ten fold change of $[K^+]_i$ only produced a change of 5 mv in the resting potential (See Fig. 1); (2) the resting potential observed at low $[K^+]_o$ cannot be explained by the term $P_{Na}[Na^+]_o$. At $[K^+]_o$ = 0 or 1 mM, a 40 fold change of $[Na^+]_o$ was found to have no effect on the resting potential (see Fig. 2). These observations do not support the prediction of the diffusion potential equation.

2. **Pulsed Nuclear Magnetic Resonance Studies of Squid Giant Axon;** cont'd on p. 2

We have measured the spin-lattice relaxation time (T_1) and spin-spin relaxation time (T_2) of water protons in squid giant axons and extruded axoplasm with a pulsed NMR technique called spin-echo. All measurements were done with a spin-lock CPS2 Spectrometer. There are two unique features of this study: Firstly, this is the first NMR study of a single fully differentiated cell; and secondly, this study offers a direct test for an interpretation which proposes that the shortening of relaxation times in biological systems is caused by the magnetic field inhomogeneity arising from the susceptibility difference between the membranes and the cytoplasmic water. The relaxation effect of membrane on the cytoplasmic water can be evaluated by comparing the relaxation times of the axon with those of the axoplasm. The results of measurements showed the following. First, the T_1 and T_2 of water proton in axon are significantly reduced in comparison to that of sea water. Secondly, the relaxation times are almost the same between the axon and the axoplasm. This indicates that the susceptibility difference between the membrane and water has a negligible effect in shortening the T_2 of water protons. Thirdly, a dead axon kept in sea water at 2°C for over one day has a longer T_2, indicating that the axoplasm in the living axon is more "structured." Fourthly, the extruded axoplasm stored in a glass tube for several days at 2°C gives similar relaxation times as that of fresh axoplasm. This suggests that the change of the structure of axoplasm must depend on the exchange of electrolyte ions with the external environment.

3. Studies of Na^{23} Nuclei in Skeletal Muscle by Fast Fourier Transform NMR and Spin-Echo NMR.

Sodium in skeletal muscle of mature and immature rats was studied with Fast Fourier Transform (FFT) nuclear magnetic resonance (NMR) and spin-echo NMR techniques. It was found that the amount of so-called "NMR-visible sodium" in muscle, determined from the area under the muscle sodium spectrum, does not reflect the concentration of the mobile sodium ions. The muscle Na^{23} spectra can be fitted with two Lorentzian curves with different line widths centering at the same resonance frequency. We also have used the spin-echo method to measure the spin-lattice relaxation time (T_1) and spin-spin relaxation time (T_2) of muscle sodium. Our data indicated that the T_1 curve follows a simple exponential decay, while the T_2 curve is complex and can be fitted with a double exponential function. Using the model of Hubbard, we have obtained quantitative information about the physical characteristic of the muscle sodium nuclei. We found that the reduction of the relaxation times of sodium is not caused by exchange of a large volume of "free" sodium with a small volume of "bound" sodium. All of the sodium ions seem to associate with the charged-sites of the biomacromolecule, and the correlation time of this association was estimated to be between 10^{-8} to 10^{-5} second. The average distance between the ion and the charged site also was estimated to be 4.5 Å to 14 Å.

4. Studies of Ion Competition Between Na^+ and K^+ Ions in the Pathway of Early Conductance (i.e., "Na^+ Channel") in Squid Giant Axon.

The ion competition between Na^+ and K^+ in the pathway of early conductance (i.e., "Na^+ channel") was studied by examining the magnitude of the early current (under voltage-clamp conditions) as a function of concentration gradients of sodium and potassium ions. Using a double perfusion technique, the concentrations of Na^+ and K^+ were controlled both at the inside and at the outside of the axon. For simplicity of interpretation, we chose to study the outward current under conditions where the artificial sea water contains no Na^+ ions (Na^+ is being replaced by choline ion). Three techniques were used to separate the early outward current from the delayed outward current: (1) We used a 20 millisecond prepulse (of 60 mv hyperpolarization) to enhance the magnitude of the early current; (2) 20 mM of tetraethylamonium (TEA) were applied inside of the axon so that the delayed current was suppressed; (3) We used Cs^+ ions to partially replace some of the K^+ ions so that the delayed current was reduced. The preliminary results indicate that the $Na^+ - K^+$ competition is not of a linear fashion, and the observed results are sensitive to the method of ion substitution. The current density (J) passing through this early "channel" varies with ionic concentrations, $[K]_i$ and $[Na]_i$ in a peculiar way. J appears to be a linear function of $[Na]_i$ while the $[K]_i$ dependence of J deviates significantly from a linear function. (See Fig. 3.)

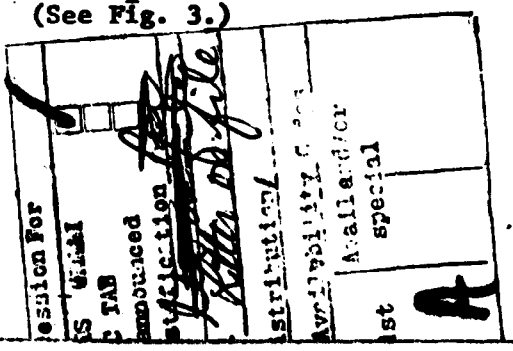

5. Study of Kinetics of Early Current and Its Concentration Dependency--Development of a TTX (Tetrodotoxin)-Subtraction Method.

In order to study the time course of the current going through the early conductance channel, one must completely abolish all other currents (such as leakage current, capacitive current, delayed current, etc.). Utilizing a digital computer and taking advantage of the specific current-blocking property of the neurotoxin, tetrodotoxin, (TTX), we have developed a TTX-subtraction method to study the time course of the early current. It is known that 4×10^{-7} M of TTX in the external solution can block completely the early current, while other current (including the delayed current) are not affected. If one measures the membrane current without TTX first and then repeats the same measurement with TTX, one can obtain the early current by subtracting the membrane current with TTX from the membrane current without TTX.

A sample record of this TTX-subtraction method is given in Fig. 4. In Fig. 4A, the membrane current measured at V = 80 mv without TTX is shown as the top trace. The membrane current measured after TTX is added is shown as the bottom trace. It is clear that the early transient current is blocked completely by TTX, while the delayed current is not affected. In Fig. 4B, the early current is obtained by taking the difference of the two current traces in Fig. 4A. The early current rises quickly after the axon is depolarized. It reaches a peak and decreases slowly toward zero. In our preliminary study, we found that the early current fits a m^8h^2 time time course (where m is an increasing exponential function and h is a decreasing exponential function), instead of a m^3h time course as originally suggested by Hodgkin and Huxley. (See Fig. 5) The cause of this discrepancy is being investigated. It is possible that our technique is more discriminating than that available to Hodgkin and Huxley, and therefore, we can determine the curve-fitting function more accurately. Alternatively, the outward early current may have a different time course than that of the inward sodium current, based on which the m^3h kinetics originally was determined.

In our preliminary study, the time course of the early current was found to vary with internal potassium concentration. A sample record of two early current traces measured at different $[K]_i$ is shown in Fig. 6. The early current measured at $[K^+]_i$ = 400 mM has a faster rising phase. The early current measured at $[K^+]_i$ = 200 mM is definitely slower. The difference in the falling phase of the early current with different $[K^+]_i$ is even more prominent. Fig. 6C shows a sample record of three early currents measured at $[K^+]_i$ = 400, 200 and 100 mM. ($[Na^+]_i$ = 50 mM in all three cases.) The early current decreases much faster at higher $[K^+]_i$.

Our findings that $[K]_i$ affects both the magnitude of the early conductance and the time course of the opening and closing of the conductance pathway are unexpected in the present models of "channel". Our findings imply

that the conduction pathway contains structures of ion-exchange properties. A detailed analysis of this ion-exchange effect will allow us to obtain a better understanding of the ionic conductance mechanism in excitable cells.

CAPTION OF FIGURES

Fig. 1 The resting potential of the perfused axon is plotted as a function of the internal K^+ concentration. The external K^+ concentration was 1 mM ($[Na^+]_o$ = 435 mM). The data represented by "0" were obtained when the internal ionic strength was kept constant (i.e., $[K^+]_i + [Na^+]_i$ = 400 mM). The data represented by "Δ" were obtained when $[K^+]_i$ was replaced by sucrose ($[Na^+]_i$ was kept at a constant of 50 mM). The solid line is the fitting of the GHK equation.

Fig. 2 The resting potential of the squid axon is plotted as a function of $[Na^+]_o$. $[K^+]_o$ was kept at 1 mM for data represented by "o". All other data were obtained when $[K^+]_o = 0$. The internal ionic concentrations were those of the intact axoplasm. The solid line is the prediction of the GHK equation. The dotted line is a constant potential fit.

Fig. 3 The current density (J) at the peak of the early conductance is plotted versus the $[Na^+]_i$ and $[K^+]_i$. Both $[Na^+]_o$ and $[K^+]_o$ were zero. The axons were depolarized from a holding potential of -60 mv to a depolarizing potential of +120 mv. A conditioning pulse of 20 msec long and -60 mv in amplitude was applied to enhance the early conductance. The data were obtained from a large number of measurements involving various axons. The value of J, therefore, was normalized. These measurements were made at 5^o C.

Fig. 4(A) The upper trace shows a sample record of membrane current when no TTX was applied. The lower trace shows the membrane current of the same axon under identical condition when 4×10^{7} M of TTX was added. The data was obtained when $[Na^{+}]_i$ = 50 mM and $[K^{+}]_i$ = 400 mM. Both $[K^{+}]_o$ and $[Na^{+}]_o$ were zero. The membrane potential was changed from -60 mv to + 80 mv in this measurement. A digital signal subtraction technique was used to get rid of the capacitive current and the leakage current. The temperature was $5^{o}C$.

(B) The time course of the early current is obtained by taking the difference between the two current traces in Fig. 4A. The delayed current is identified to the current trace with TTX (in Fig. 4A).

Fig. 5 The time-course of the early current using a digitalized TTX - subtraction technique is shown in this figure. The best computer fits of two theoretical curves $m^{8}h^{2}$ and $m^{3}h$ were also plotted. It appears that the fitting of $m^{8}h^{2}$ is much better than the fitting of $m^{3}h$.

Fig. 6 The time course of early currents measured at different $[K^{+}]_i$ is shown in this figure. (A) A sample time course of the early current using a TTX-subtraction method. (B) The rising phase of two early current traces with $[K^{+}]_i$ = 400 mM at 200 mM ($[Na^{+}]_i$ = 50 mM). The kinetics of the current trace with higher $[K^{+}]_i$ rises at a faster pace. Each dot represents current measured at 10 microseconds intervals. (C) The falling phase of three early current traces with $[K^{+}]_i$ = 400, 200, and 100 mM are shown. The current falled faster at higher $[K^{+}]_i$.

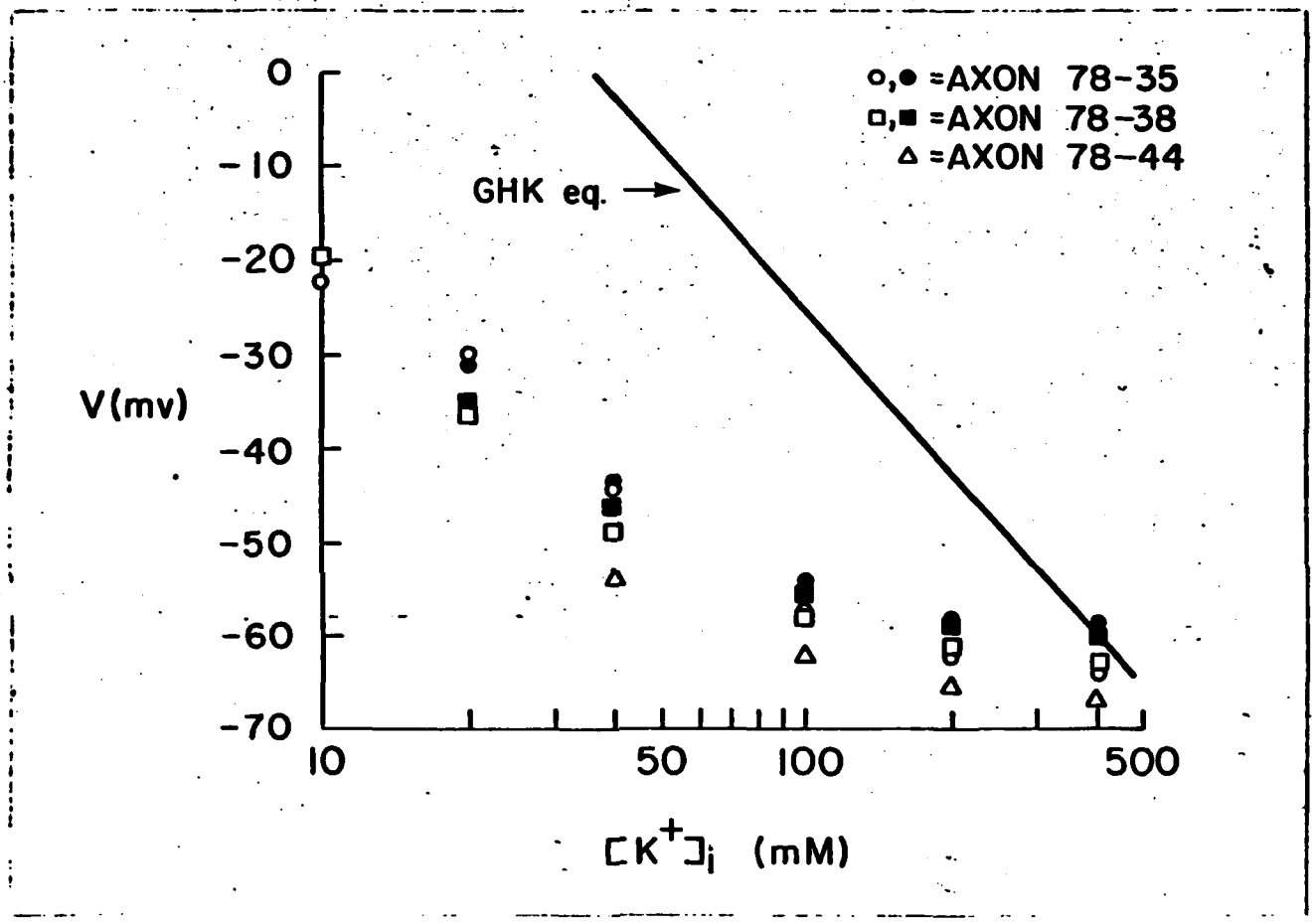
0
-10
-20
-30
-40
-50
-60
-70
V(mv)
10
50
100
500
[K+]i (mM)
GHK eq.
o,● =AXON 78-35
□,■ =AXON 78-38
△ =AXON 78-44

Figure 1

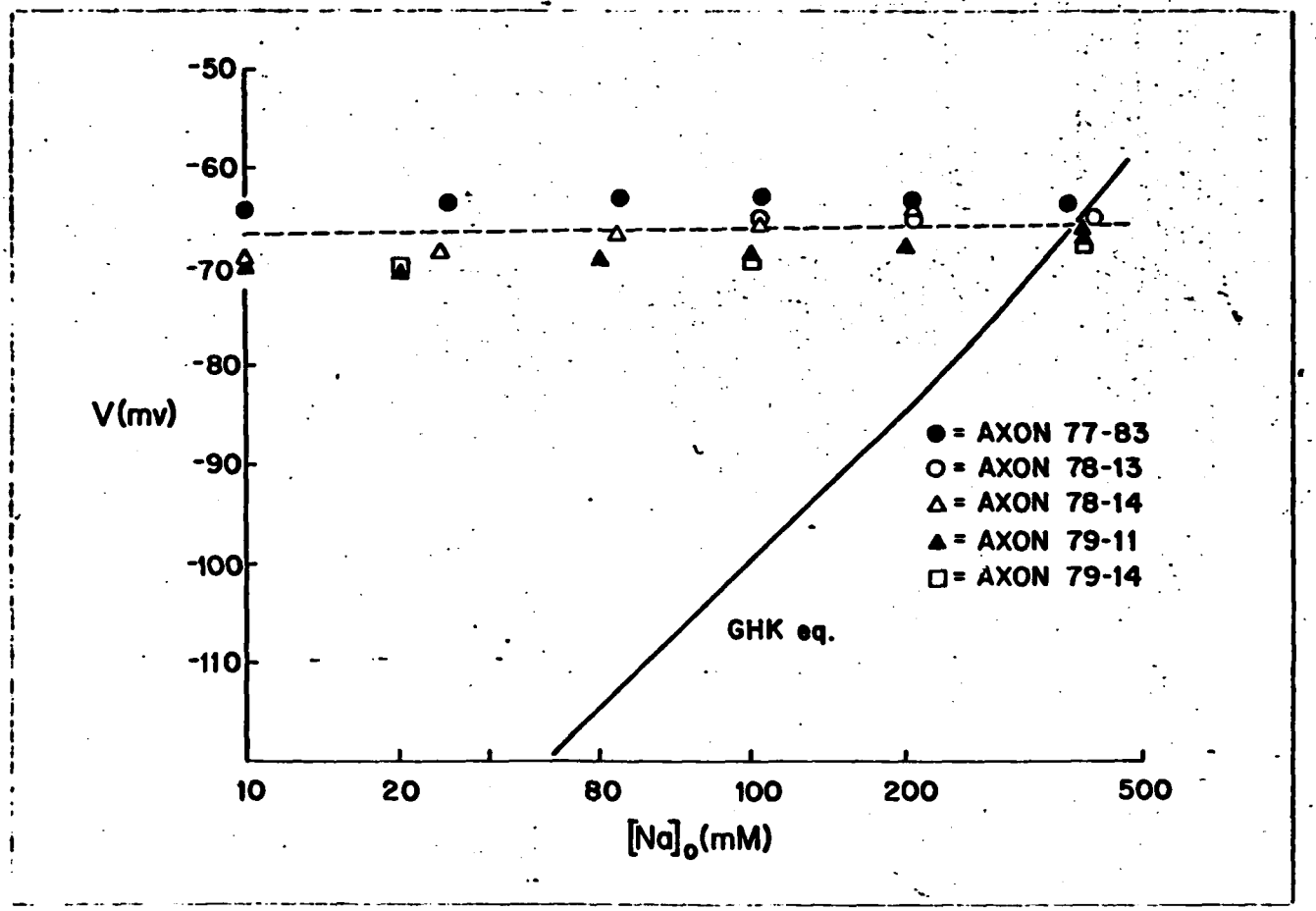
-50
-60
-70
-80
-90
-100
-110
V(mv)
10
20
80
100
200
500
[Na]o(mM)
● = AXON 77-83
○ = AXON 78-13
△ = AXON 78-14
▲ = AXON 79-11
□ = AXON 79-14
GHK eq.

Figure 2

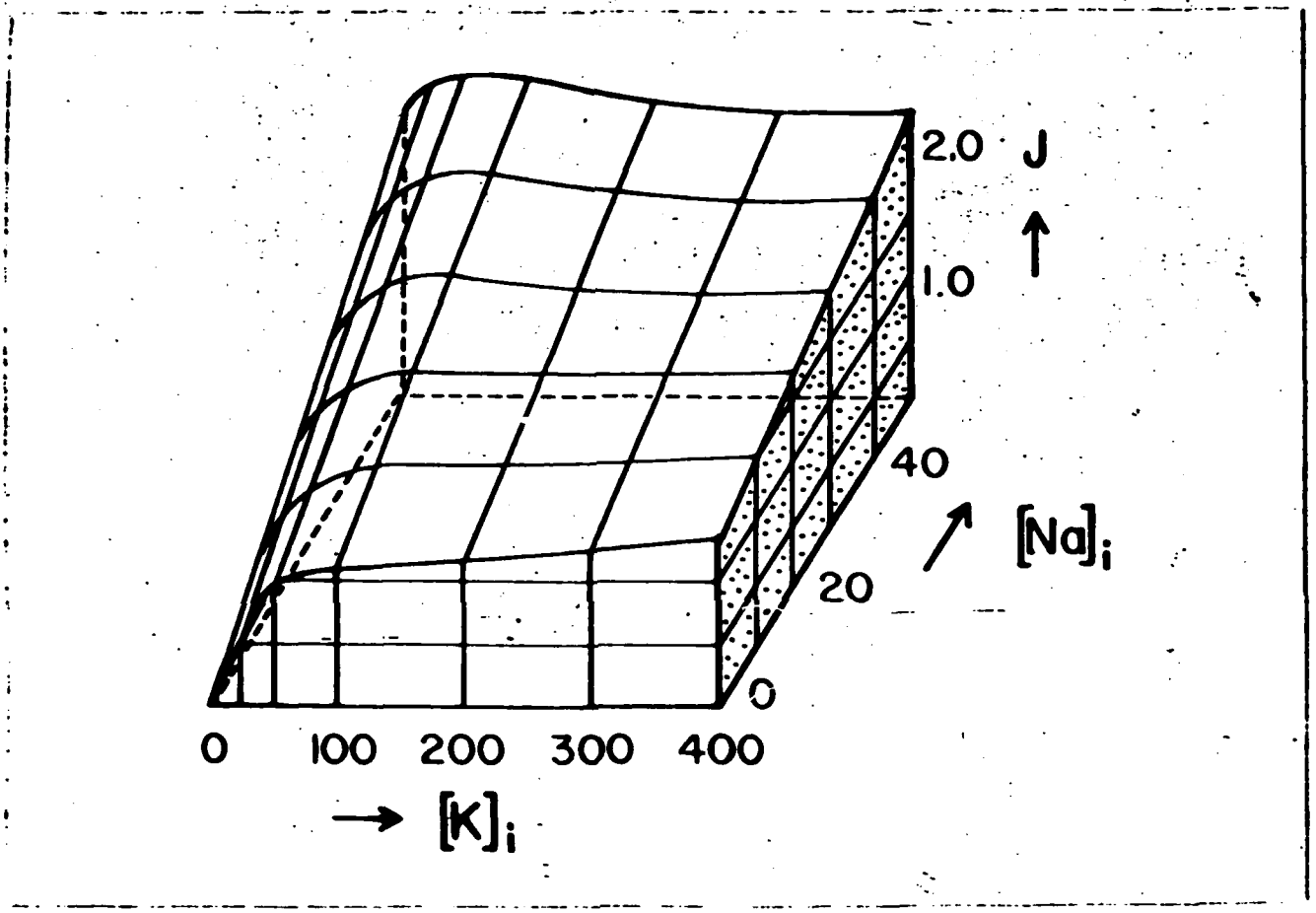

Figure 3

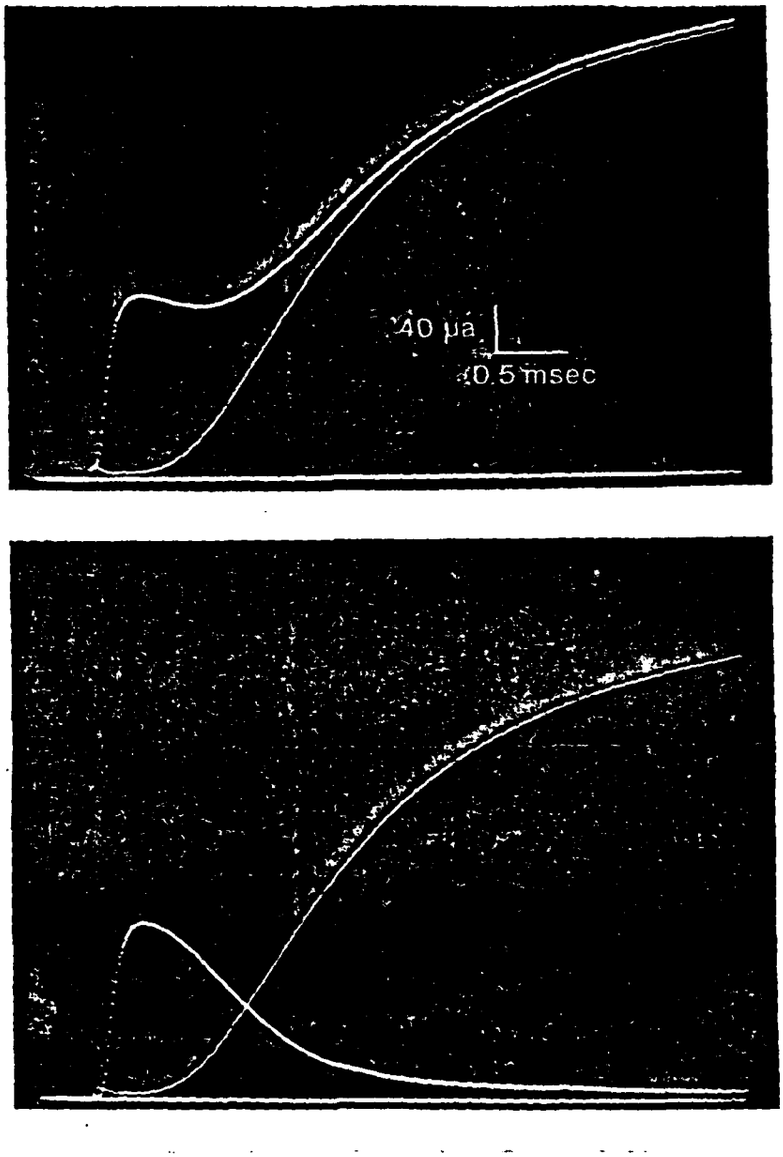

Figure 4

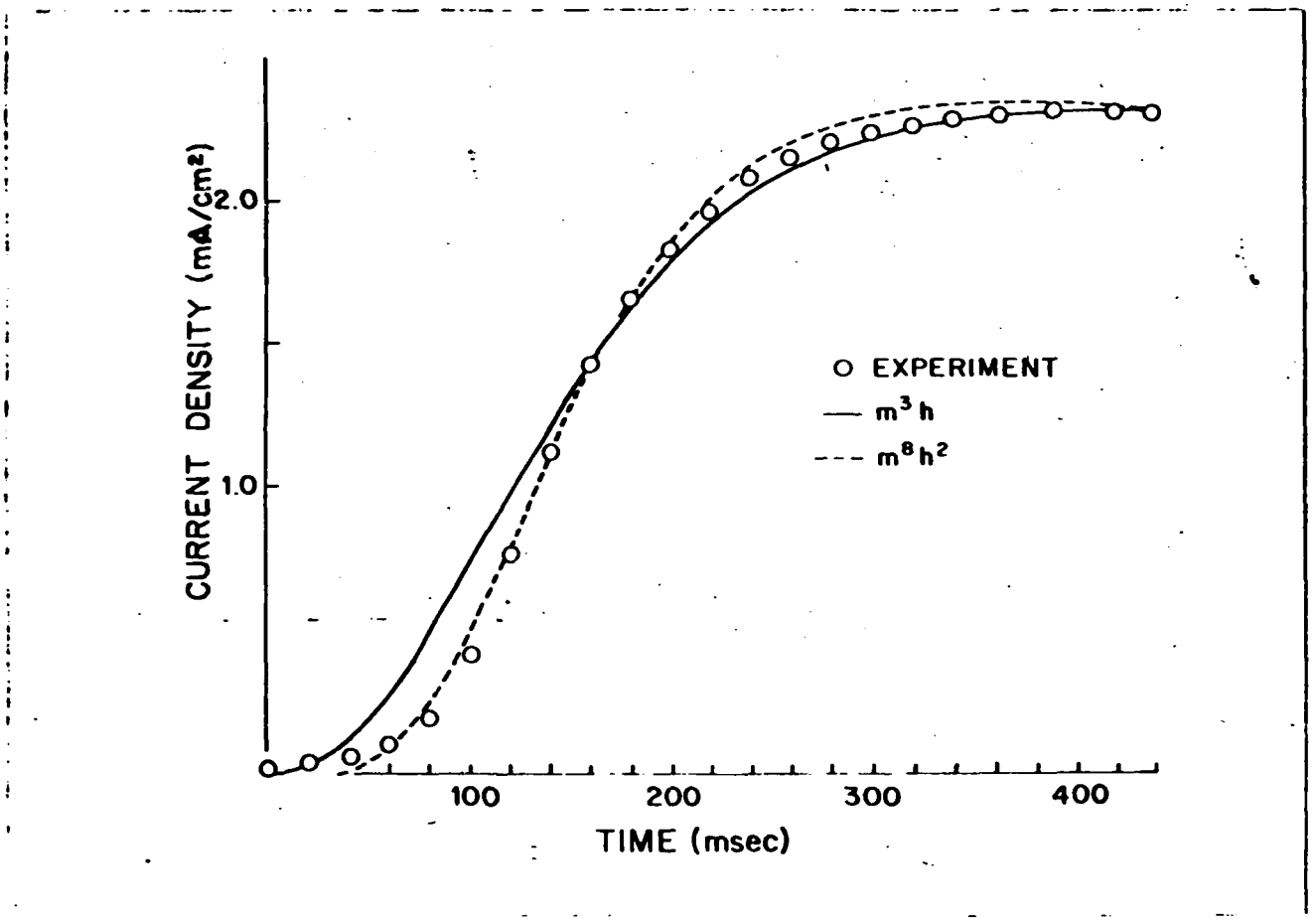
CURRENT DENSITY (mA/cm²)
2.0
1.0
100
200
300
400
TIME (msec)
O EXPERIMENT
m³h
m⁸h²

Figure 5

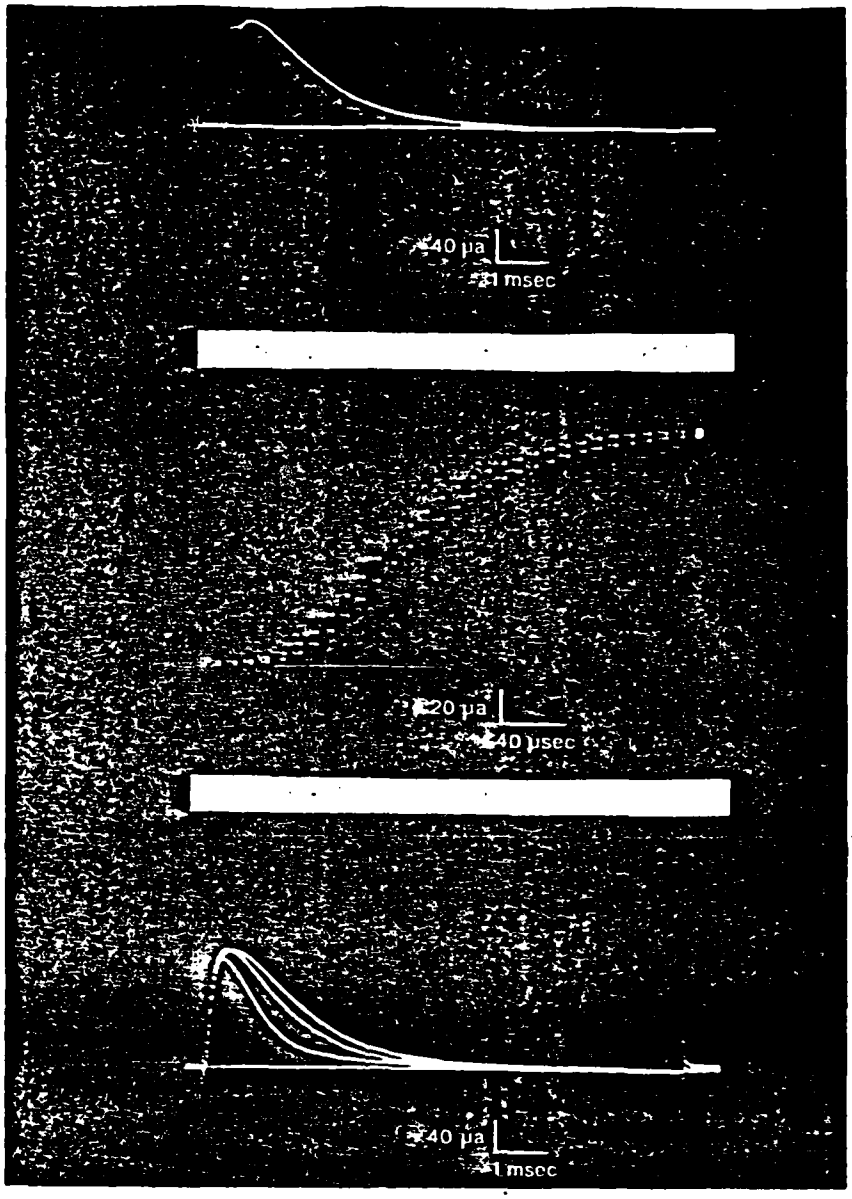

Figure 6


DATE
FILME
8-8